



Global geomagnetic responses to the IMF B_z fluctuations during the September/October 2003 high-speed stream intervals

Ezequiel Echer¹, Axel Korth², Mauricio José Alves Bolzan³, and Reinhard Hans Walter Friedel⁴

¹Space Geophysics Division, National Institute for Space Research (INPE), 12227-010, Sao Jose dos Campos, SP, Brazil

²Planetary Department, Max-Planck-Institut für Sonnensystemforschung, Justus-von-Liebig Weg 3, 37077 Göttingen, Germany

³Space Physics Laboratory, Federal University of Goiás, 78804-020, Jataí, GO, Brazil

⁴Los Alamos National Laboratory, National Security Education Center (NSEC-CSES), MS-T001, Los Alamos, NM 87545, USA

Correspondence to: Ezequiel Echer (ezequiel.echer@gmail.com)

Received: 6 May 2016 – Revised: 12 April 2017 – Accepted: 6 June 2017 – Published: 21 July 2017

Abstract. In this paper, we follow the coupling from the solar wind to the Earth's magnetotail, geosynchronous orbit, auroral zone and to the ground, during periods of Alfvénic fluctuations in high-speed solar wind streams (HSSs) and their corotating interaction regions (CIRs). We employ cross-wavelet analysis of magnetic field, particle flux and auroral electrojet (AE) index data for the HSSs of September and October 2003. Our results show a remarkably consistent periodic response among all of these regions and across multiple substorm indicators, indicating a possible driven substorm response of the global magnetosphere to the solar wind interplanetary structures. Across the seven intervals studied we find a range of periodic responses from 1.8 to 3.1 h, which is consistent with the 2.75 h peak of the Borovsky et al. (1993) statistical study of inter-substorm periods.

Keywords. Magnetospheric physics (magnetotail; solar wind–magnetosphere interactions; storms and substorms)

1 Introduction

It has been known for a long time that the main cause of geomagnetic activity is the enhanced solar wind–magnetosphere energy coupling through the magnetic reconnection mechanism when the interplanetary magnetic field (IMF) has a southward-directed component (Dungey, 1961; Russell et al., 1974; Akasofu, 1981; Gonzalez et al., 1994; Echer et al., 2005). Geomagnetic activity consists of several types of disturbances, the most widely studied being geomagnetic

storms, substorms and HILDCAAs (high-intensity, long-duration, continuous AE activity; Gonzalez et al., 1994; Guarnieri et al., 2006a; Hajra et al., 2013).

The interplanetary causes of the variations of the IMF B_z component and the geomagnetic activity are known to change with the solar cycle. For geomagnetic storms, the interplanetary remnants of coronal mass ejections (ICMEs) are dominant around solar cycle maximum phases, while during the declining and solar minimum phases, corotating HSSs and their corotating interaction regions (CIRs) are responsible for most of the storm/substorm activity (Burlaga and Leping, 1977; Crooker and Cliver, 1994; Lindsay et al., 1995; Baker, 1996; Gonzalez et al., 1999, 2007, 2011; Kamide et al., 1998; Gosling and Pizzo, 1999; Richardson et al., 2000; Alves et al., 2006; Echer et al., 2008, 2013).

During the declining and minimum phases of solar cycles, coronal holes (CHs) typically extend to lower heliographic latitudes and their high-speed streams (HSSs) reach the ecliptic plane. CIRs are formed by the interaction of fast solar wind streams and the ambient, slower solar wind stream (Sheeley and Harvey, 1981; Pizzo, 1982; Balogh et al., 1999; Tsurutani et al., 2006; Cranmer, 2009). At large distances (> 2 AU) from the sun, CIRs are bounded by fast forward and fast reverse shocks (Smith and Wolfe, 1976). However, at 1 AU the shocks that will eventually bound CIRs are usually not fully formed (Tsurutani et al., 1995; Gonzalez et al., 1999). Since coronal holes are long-lived structures, they can persist for more than one solar rotation, and the HSSs emanating from the same region reappear at intervals of approxi-

mately 27 days (solar synodic rotation period; Sheeley et al., 1976; Tsurutani et al., 1995; Guarnieri et al., 2006a, b).

A very important aspect of these fast streams is that they are embedded within Alfvén waves (Belcher and Davis, 1971). These Alfvén waves are believed to be remnants of heating processes in the Sun (Hollweg, 1978). In the interplanetary data, these waves appear as large-amplitude oscillations in magnetic field components, well correlated with the oscillations of the velocity components (in the same direction; Belcher and Davis, 1971; Tsurutani et al., 1995, 2011). These Alfvén waves, with intermittent negative IMF B_z and large IMF y component $|B_y|$, may lead to significantly enhanced magnetospheric convection.

Substorms are transient magnetospheric processes where the solar wind–magnetosphere interaction energy is dissipated mainly in the night-side auroral ionosphere (Akasofu, 1964; Rostoker et al., 1980). Substorms are much smaller in physical scale and energy than geomagnetic storm events. Magnetospheric substorms are initiated in the magnetotail at distances of about $20R_E$. When they occur, the auroral displays become very bright and active, there is intensification in the current flow in the magnetosphere and ionosphere, the plasma sheet becomes very thin in localized regions and hot plasma is impulsively injected into the inner magnetosphere (Burch, 1987). Some researchers have found that a southward turning of the IMF and magnetic reconnection is the energy transfer mechanism predominant for substorms as well (Tsurutani and Meng, 1972; Akasofu, 1981). The question of what external or internal events cause or trigger recurring periodic substorms has been one of the fundamental issues of substorm research, and one on which there is yet no consensus. Individual substorm occurrence has been linked to northward turnings of the IMF at the end of intervals of southward IMF (Blanchard et al., 2000). However, there is some dispute over this claim (Morley and Freeman, 2007; Freeman et al. 2009). While random or isolated substorms form the largest class of events, periodic substorms are often observed with inter-substorm times of around 3 h (Borovsky et al., 1993). Periodic activity, such as during sawtooth events, has been directly correlated with corresponding solar wind dynamic pressure enhancements (Henderson et al., 2006). Other works suggest that sawtooth events can be viewed as a magnetospheric mode similar to steady magnetospheric convection (SMC) intervals except that for sawtooth events, the flow of energy from the solar wind into the magnetosphere becomes too large to dissipate without the periodic occurrence of substorms (Sergeev, 1996 and references there in). They further suggest that the quasi-periodicity arises because the magnetosphere may only become susceptible to external or internal triggering after it has been driven beyond a stability threshold. This has been further demonstrated by the minimal substorm model of Freeman and Morley (2004). This can account for the existence of a higher rate of possible external triggers (in the IMF or solar wind) than actual substorm events, with triggers arriving faster than the time

needed for the magnetosphere to reach its stability threshold. The magnetosphere may be selectively responsive to such a structure (Borovsky et al., 1993; Henderson et al., 1996) only when enough energy has been loaded into the system. Pulkkinen et al. (2007) have shown that $\sim 30\%$ of the storm time substorm-like activations and 20% of the sawtooth oscillations have associated solar wind or IMF triggers and that this triggering is more likely during high solar wind pressure and fluctuating IMF intervals.

Two major substorm models have been developed: the first one is the near-Earth neutral line model (NENL; Baker et al., 1996), which assumes that reconnection takes place between the oppositely directed field lines above and below the current sheet at a distance of about $2\text{--}30 R_E$ (this is considered near-Earth as opposed to the distant tail reconnection), resulting in fast plasma flow transferring disturbances to the inner magnetosphere. The second one is the cross-field current instability (CCI; e.g., Lui, 1996; Lui et al., 2008) model, in which the substorm is initiated as a current driven plasma instability that creates the substorm current wedge, and reconnection may play no role at all, or only a secondary role in creating the down-tail plasmoid. This model places the onset region much closer to the Earth than the NENL model ($\sim 6\text{--}15 R_E$).

Recently substorms have been studied with multi-spacecraft missions to evaluate these substorm models: Cluster (e.g., Baker et al., 2005; Lui et al., 2008) and THEMIS (e.g., Angelopoulos et al., 2008). Furthermore, complex system and entropy studies have been conducted on the solar wind–magnetosphere coupling (e.g., Balasis et al., 2009). However, these studies have shown support for both the NENL and CCI models; there is still no agreement on which is the most dominant mechanism.

The year 2003 was dominated by large coronal holes and their very powerful HSSs (Kozyra et al., 2006) and substorm activity (Tanskanen et al., 2005). The 2003 HSS events have been studied by other workers (Korth et al., 2006; Lee et al., 2006; Lyons et al., 2009; Tsurutani et al., 2011; Bolzan et al., 2012). However, a global solar wind–magnetosphere interaction study during 2003 HSS intervals is still outstanding.

The aim of this paper is to study the geomagnetic effects of Alfvénic fluctuations in CIRs and their driving HSSs. We intend to study the HSS effects by following their signatures from the interplanetary medium to the Earth's magnetotail, then to geosynchronous orbit and finally down to the ground. In order to establish connectivity between the signatures observed in these locations, we use the cross-wavelet analysis technique to identify the main frequencies where the cross-correlation is highest, which indicates a strong energy coupling and modulation of the magnetosphere by IMF B_z variations leading to substorms.

2 Methodology of analysis and data

2.1 Data

Solar wind data are derived from the ACE (Advanced Composition Explorer) solar wind plasma and magnetic field instruments (McComas et al., 1998; Smith et al., 1998), measured at the L1 position. These 1 min averaged data are used to identify the HSS intervals. ACE solar wind IMF B_z data are time-shifted to the Earth's bow shock and were obtained from the National Aeronautics and Space Administration (NASA) Goddard Space Flight Center (GSFC) Omniweb server (<http://omniweb.gsfc.nasa.gov/>). Geomagnetic activity is evaluated using the 1 h Dst and the 1 min geomagnetic auroral electrojet (AE) indices (Rostoker, 1972), from the World Data Center for Geomagnetism, Kyoto (<http://swdcwww.kugi.kyoto-u.ac.jp/>). The AE index was originally introduced by Davis and Sugiura (1966) as a measure of the global electrojet activity in the auroral zone.

Magnetotail data are from the Cluster mission fluxgate magnetometer (FGM; Balogh et al., 2001) instrument. Data were taken from the C4 spacecraft only and were obtained through the Cluster active archive, from the European Space Agency (ESA) server (<http://caa.estec.esa.int>). We further used electron and proton fluxes from the Cluster energetic particle spectrometer RAPID (Research with Adaptive Particle Imaging Detectors; Wilken et al., 2001) in the energy range between 30 and 100 keV and 50 to 1500 keV, respectively. The low energy range is covered by the Cluster CODIF (Composition and Distribution Function) analyzer in the energy range from 30 eV to 40 keV. CODIF is one of the sensors of the CIS (Cluster Ion Spectrometry) instrument (Reme et al., 2001).

Electron fluxes at geosynchronous orbit were taken from the synchronous orbit particle analyzer (SOPA) instrument onboard the Los Alamos National Laboratory (LANL) spacecraft 1991-080 (Bame et al., 1986). SOPA measures electrons from ~ 48 keV to ~ 1.5 MeV, but this study only used the first three differential channels (48–69, 69–102, 102–150 keV).

Ground-based magnetometer data were taken from the following locations: Abisko (ABK) at 68.36° N, 18.82° E, geomagnetic latitude 66.10° N; Barrow (BRW) at 71.32° N, 156.62° W, geomagnetic latitude 69.78° N; College (CMO) at 64.87° N, 147.86° W, geomagnetic latitude 65.49° N; and Narsarsuaq (NAQ) at 61.20° N, 45.40° W, geomagnetic latitude 69.65° N. The stations are located in the auroral zone at various longitudes (near equally separated). The high-resolution (1 min) data were downloaded from the World Data Center (WDC) of Geomagnetism, Kyoto. The disturbance in the horizontal component, H , is determined after the solar quiet variation has been removed.

For our analysis intervals, simultaneous measurements are required in the tail of the magnetosphere and at the ACE spacecraft when detecting HSSs. Table 1 shows the seven

intervals used in this study, four in September 2003 and three in October 2003. The selection intervals are mainly dictated by the Cluster orbit and ranged from 24 to 40 h. Cluster is near the central plasma sheet for a subset of the whole tail crossing. However, we have used a longer interval around the plasma sheet in order to have a high confidence level/statistical significance for the periods found in the wavelet analysis. Geosynchronous and ground-based data were available continuously for our study interval.

2.2 Wavelet and cross-wavelet analysis

To analyze the coupling among different regions of the near-Earth space environment, we used cross-wavelet analysis applied to the time series of the data. The wavelet transform (WT) is a very powerful tool to analyze non-stationary signals. It permits the identification of main periodicities in a time series and the time evolution of each frequency (Kumar and Foufoula-Georgiou, 1997; Torrence and Compo, 1998; Percival and Walden, 2000; Balasis et al., 2006, 2012; Auchère et al., 2016; Katsavrias et al., 2016).

The WT of a discrete data series is defined as the convolution between the time series with a scaled and translated version of the wavelet function chosen. By varying the wavelet scale and translating in time, it is possible to construct a picture showing the amplitude of any characteristics versus scale (equivalent to frequency or period), and how this amplitude varies with time. Mathematically, the WT is defined as

$$W^X(a, b) = \frac{1}{a^{1/2}} \int x(t) \psi\left(\frac{t-b}{a}\right) dt, \quad (1)$$

where $x(t)$ is the time series, ψ is the wavelet function chosen and a , b are the scaling factor and translation parameter, respectively.

We used the WT in two approaches. First, we use the WT to remove the long-term trend from the time series, and second, we use the WT to perform the cross-wavelet spectrum (XWS) analysis between two time series. For more details of the first approach, see Bolzan et al. (2009). For the second approach the following must be valid: if $X(t)$ and $Y(t)$ are time series and if $W^X(a, b)$, $W^Y(a, b)$ are their WT, the XWS analysis (Torrence and Compo, 1998; Bolzan and Vieira, 2006) is given by

$$\left| W^{XY}(a, b) \right| = W^X(a, b) \cdot W^Y(a, b). \quad (2)$$

$W^Y(a, b)$ is the complex conjugate of $W^X(a, b)$ and $||$ denotes the absolute values. The wavelet function used here was the Morlet function due to their special properties in geophysical time series (Torrence and Compo, 1998; Bolzan and Vieira, 2006).

The XWS indicates the scales of higher covariance between two time series (X , Y). This analysis gives a measure of correlation between two time series as a function of the

Table 1. Magnetotail crossings studied in this work (Cluster C4 spacecraft) and cross-wavelet analysis results (major periods).

Crossing	Time	Duration	Cross-wavelet IMF B_z vs. Cluster tail B_x (h)
T1	00:00 17/09/2003 to 09:00 18/09/2003	33	1.9
T2	10:00 19/09/2003 to 10:00 20/09/2003	24	2.1
T3	18:00 21/09/2003 to 10:00 23/09/2003	40	3.1
T4	07:00 24/09/2003 to 21:00 25/09/2003	38	2.9
T5	14:00 15/10/2003 to 20:00 16/10/2003	30	2.7
T6	00:00 18/10/2003 to 04:00 19/10/2003	28	1.8
T7	06:00 20/10/2003 to 12:00 21/10/2003	30	2.4

period of the signal and its time evolution with a 95 % confidence level (Torrence and Compo, 1998).

We have used in this paper the Torrence and Compo (1998) code which is widely used in geophysical applications. For drawbacks of this code, see Auchère et al. (2016). Comments about the possible effects of white noise and red noise on the results are included in the next section.

3 Results

3.1 Description of the events

We investigate the effects of HSSs on the Earth's magnetotail during the September and October 2003 periods. For solar cycle 23, the maximum HSS activity occurred in the year 2003. During that year the largest yearly averaged energy input was measured within the last four solar cycles as given by the AE index (Kozyra et al., 2006). The period from August to December 2003 showed a series of long duration HSSs with speeds from ~ 600 to ~ 800 km s $^{-1}$ (Lee et al., 2006; Lyons et al., 2009; Tsurutani et al., 2011; Bolzan et al., 2012).

Figure 1 shows an overview plot of ACE solar wind data (speed V_{sw} , IMF magnitude B_0 , IMF B_z component and density N_p), Dst and AE geomagnetic activity indices. The intervals T1 to T7 indicated by the horizontal red lines on top of the solar wind speed panel give the periods when the Cluster C4 spacecraft crosses the magnetotail from north to south. In Table 1 the seven tail crossings from Cluster are described in detail. The columns show the intervals selected for analysis in day of year (DOY), day of month, UT and the duration of the crossings. The tail crossings lasted between 24 and 40 h.

Tail crossings T1, T2, T3 and T4 correspond to the events in September 2003 studied partially by Korth et al. (2006). They involve a recovery phase of two weak storms (Dst > -50 nT). Tail crossings T5, T6 and T7 correspond to the first period in October 2003 studied by Tsurutani et al. (2011). It is a recurrent event of the September HSS. Two moderate geomagnetic storms were observed during this interval: the first one had a peak Dst of -85 nT at 23:00 UT

on 14 October 2003, and the second one a peak Dst of -52 nT at 05:00 UT on 27 October 2003 (Echer et al., 2011). Both September and October HSSs have their solar sources identified as coronal holes. The Alfvénicity of the September 2003 HSSs was analyzed and demonstrated in Tsurutani et al. (2011).

In 2003, unusually large polar CHs stretched toward the Sun's equator, developing low-latitude extensions that persisted in some form for most of the year. Due to these low-latitude extensions of CHs, the HSS reached speeds near 800 km s $^{-1}$ (Kozyra et al., 2006). Images from the Solar and Heliospheric Observatory Extreme ultraviolet Imaging Telescope (SOHO EIT) of these large low-latitude CH can be seen in plate 1 of the Kozyra et al. (2006) paper.

Figure 2 shows the ACE IMF B_z component and the Cluster B_x component data during the tail crossings for the September 2003 HSS (DOY 259 to 269 or 16 to 26 September 2003) and for the October 2003 HSS (DOY 288 to 295 or 15 to 22 October 2003). The magnitude of B_x is an indicator when the Cluster spacecraft crosses the magnetic equator in the tail. The B_x magnetic field is positive in the northern and negative in the southern plasma sheet. B_x is further an indicator for the stretching or dipolarization of the tail field. A large change of the B_x component means that the Cluster spacecraft moves in and out of the central plasma sheet.

Figure 3 shows Cluster C4 spacecraft data for the tail crossing T2 (10:00 UT 19 September 2003 to 10:00 UT 20 September 2003). From top to bottom we plotted the Cluster C4 RAPID electron data (energy range 30–300 keV), the RAPID proton data (energy range 50–1500 keV), and the CIS CODIF proton spectrogram with its pitch angle distribution (energy range 0.03–40 keV e $^{-1}$). Further, we show FGM magnetic field data (x , y and z components in GSM coordinates, corresponding to black, green and red lines, respectively), CODIF total pressure and CODIF plasma beta (β). The B_x component of the magnetic field indicates where the Cluster spacecraft crosses the magnetic equator. B_x also points out how much the tail field is stretched. When $\beta \sim 1$, this implies that the spacecraft is in the plasma sheet, and when $\beta \ll 1$, this means that the spacecraft is in the plasma sheet boundary layer or even in the lobes.

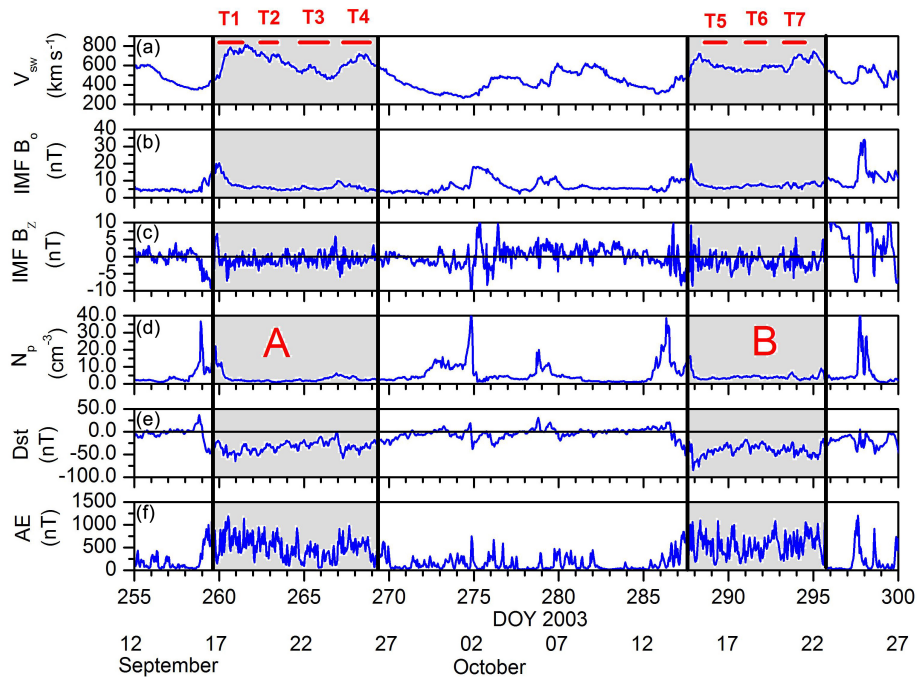


Figure 1. Panels (a) to (b) show ACE solar wind data: speed (V_{sw}), IMF magnitude (B_0), IMF B_z component (in GSM) and solar wind proton density (N_p). Panels (e) and (f) show 1 h Dst and 1 min AE geomagnetic indices. The interval is DOY 255 to 300 of 2003 (12 September to 27 October 2003). The horizontal red lines marked T1 to T7 indicate the periods corresponding to the Cluster magnetotail crossings studied in this work. Period A is the September HSS interval, and period B is the recurrent event of the September HSS.

We observe a hot and disturbed plasma sheet. The Cluster spacecraft moves in and out of the plasma sheet. In the two time intervals marked by vertical lines the spacecraft is outside the plasma sheet in the lobes. The total pressure (kinetic and magnetic) increases and decreases when the spacecraft is in the plasma sheet. During the pressure increase the magnetic field stretches and during the decrease the field dipolarizes. The pressure changes are comparable to a loading and unloading process, also called the growth and recovery phase of a substorm. During the growth phase the total pressure increases (in this event up to 0.7 nPa), the tail magnetic field stretches and the spacecraft moves out of the plasma sheet into the tail lobe. At the end of the growth phase the tail field dipolarizes or thickens and the spacecraft is back in the plasma sheet. Inside the plasma sheet we observe protons as well as electrons up to about 200 keV (RAPID top two panels). The CODIF pitch angle spectrum shows an isotropic distribution and strong fluxes at energies > 5 keV. Substorm signatures in the magnetic field component are evident for a range of latitudes either side of the Equator; in fact, it can be argued that a dipolarization signature is visible everywhere except exactly at the geomagnetic equator.

3.2 Cross-wavelet results

In order to investigate the coupling power from the solar wind into the magnetotail, we have calculated the cross-

wavelet power between the ACE B_z component and the Cluster B_x component data.

Figure 4 shows the cross-wavelet spectra between ACE IMF B_z component and the Cluster C4 B_x component for (a) 19–20 September 2003 tail crossing (T2) and for (b) 15–16 October 2003 tail crossing (T5). The cross-correlation plots indicate the Universal Time (UT) on the x axis and the periods (or frequencies) on the y axis. The color bar is indicative of the correlations. The red color indicates a strong correlation and the blue color a weak correlation. The color bar is the same for both correlation plots. The cross-correlation has its highest power at the 2.1 h peak for the T2 crossing and less power at the 2.7 h peak for the T5 crossing. We use here Cluster data from very similar positions in the magnetotail, and the delay with respect to ACE shifted data should be more or less equal. A $1 R_E$ variation in the tail position represents $\sim 0.4\%$ of the total distance to L1. At any rate, since we are interested in the recurrence periodicities of substorms, the absolute time delay from the solar wind input driver measurements is of little importance.

In Fig. 5 we show the coupling power between the solar wind region (ACE B_z) and the auroral region given by the AE index. The cross-wavelet spectrum is shown between ACE IMF B_z component data and AE index for 19–20 September 2003 tail crossing (T2) and for 15–16 October 2003 tail crossing (T5). The maximum cross-correlations are at 2.3 h for the T2 crossing and at 3.3 h for the T5 crossing. It can

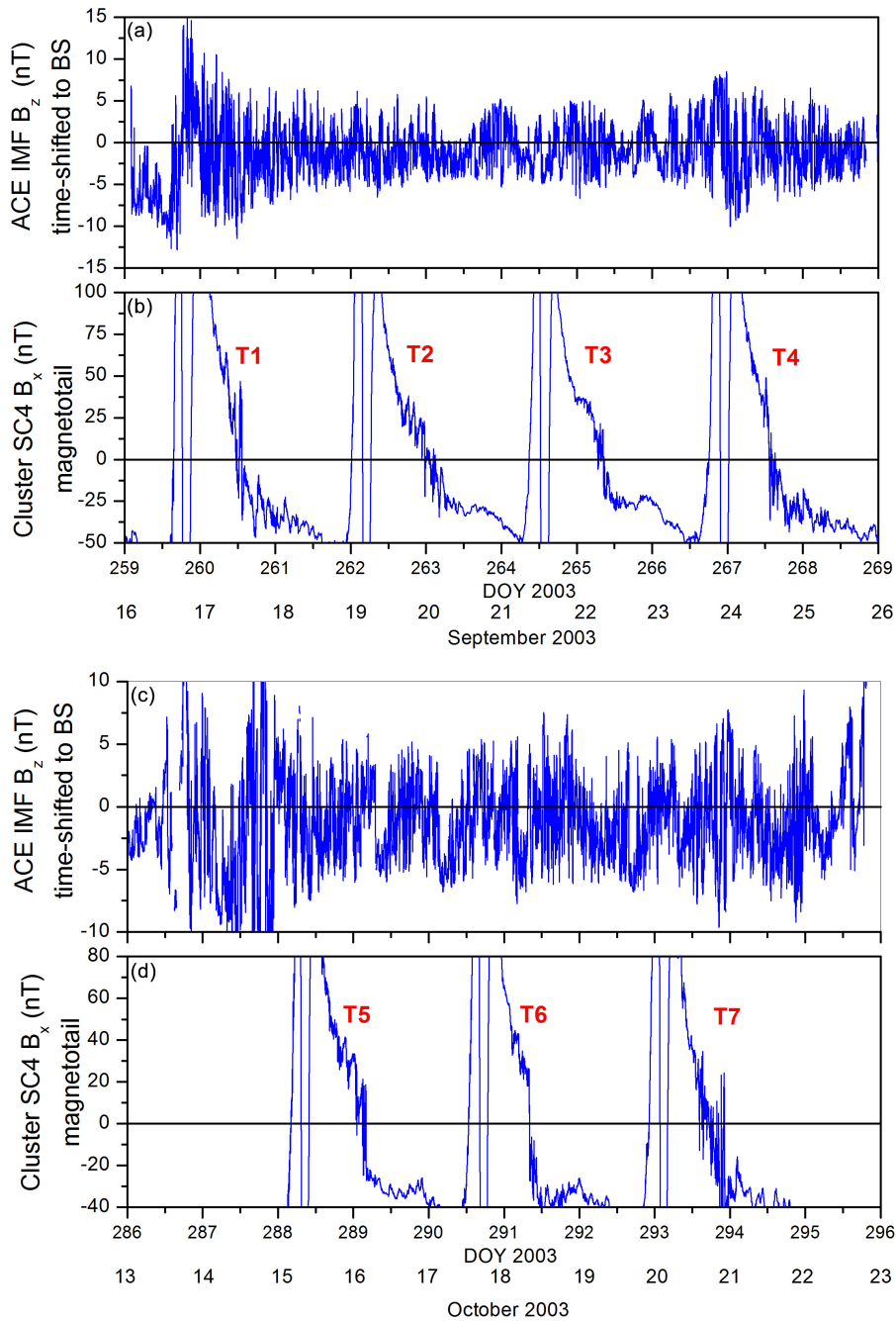


Figure 2. Panel (a) ACE 1 min IMF B_z component data propagated to the Earth's bow shock. (b) Cluster C4 B_x component data. Time period is DOY 259 to 269 (16 to 26 September 2003). (c) ACE 1 min IMF B_z component data propagated to the Earth's bow shock. (d) Cluster C4 B_x component data. Time period is DOY 288 to 296 (15 to 22 October 2003).

be noted that differences are found in the magnitude of the cross-correlations displayed in the color bars between Figs. 4 and 5. This is due to the much higher magnetic field in the auroral zone and therefore in the power (nT^2) of the global spectra.

Figure 6 gives the coupling power between the tail region (Cluster B_x) and the auroral zone (AE index) for the events

on 19–20 September 2003 and on 15–16 October 2003. The maximum cross-correlations are of the same size as in Figs. 4 and 5, here 2.6 h for the T2 crossing and 2.9 h for the T5 crossing. The time delay between tail and auroral activities are typically in the range of minutes so that the time variation should be negligible. The release of stored energy in the

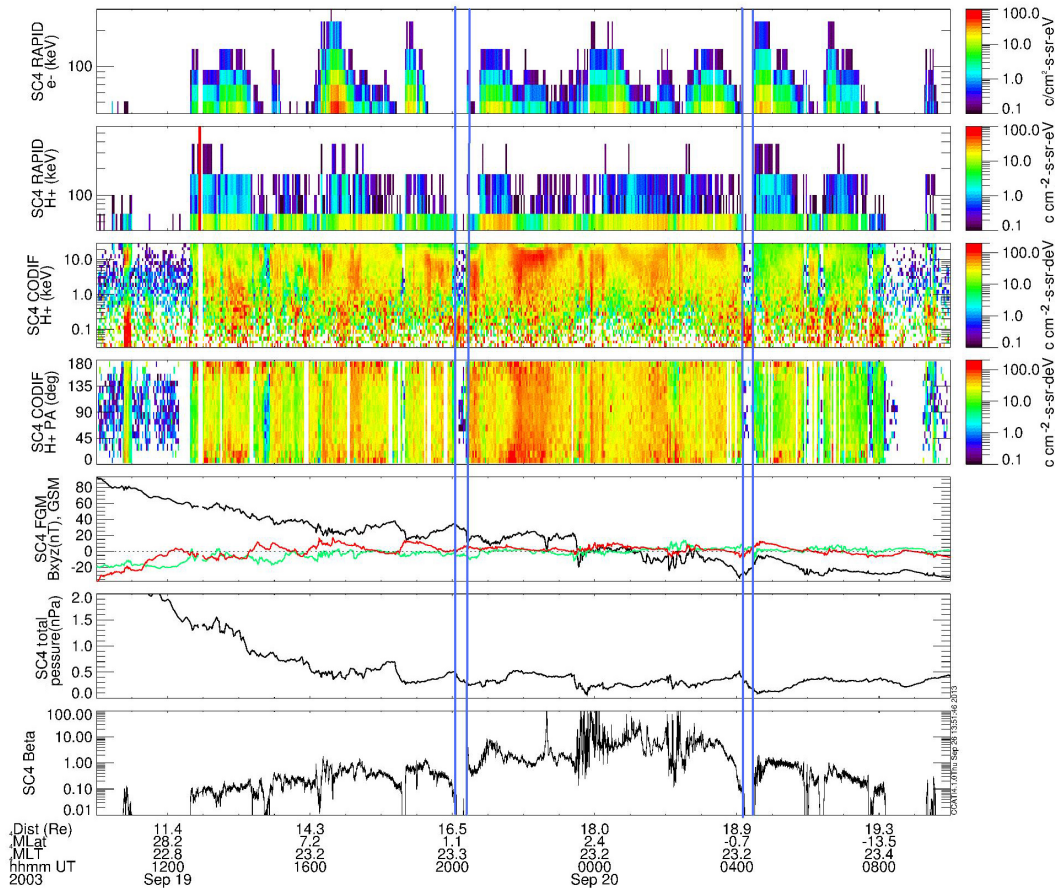


Figure 3. Cluster C4 spacecraft data for the tail crossing T2 (10:00 UT, 19 September 2003 to 10:00 UT, 20 September 2003). Panels are Cluster C4 RAPID electron energy spectrum, RAPID H+ energy spectrum, CODIF H+ energy spectrum, CODIF H+ pitch angle spectrum, FGM magnetic field components (x , black line; y , green line; z , red line) in GSM coordinates, CODIF total pressure and CODIF plasma beta.

magnetotail to the auroral zones occurs about 15 min after the IMF has turned southward (Tsurutani and Meng, 1972).

All these factors are represented in the width of the cross-wavelet analysis peaks.

Figure 7 shows the cross-wavelet spectra between Cluster B_x component data in the tail and LANL fluxes of energetic electron data at the geosynchronous orbit for three energy channels between 48.15 and 149.45 keV for the 19–20 September 2003 tail crossing (T2) and for the 15–16 October 2003 tail crossing (T5). The maximum cross-correlation is at 2.2 h for the T2 crossing and at 3.5 h for the T5 crossing.

Figure 8 shows the cross-wavelet spectra between LANL electron fluxes between 48.15 and 149.45 keV and Cluster RAPID > 100 keV electron fluxes for 19–20 September 2003 tail crossing (T2) and for 15–16 October 2003 tail crossing (T5). The maximum cross-correlation is at 2.3 h for the T2 crossing and at 2.9 h for the T5 crossing.

Figure 9 shows the cross-wavelet spectra between Cluster B_x component data and ABK ground station geomagnetic data for 19–20 September 2003 tail crossing (T2) and for

15–16 October 2003 tail crossing (T5). The maximum cross-correlation is at 2.4 h for the T2 crossing and at 3.3 h for the T5 crossing.

3.3 Summary of wavelet and cross-wavelet results

Table 1 shows a summary of the major periods found in the cross-wavelet spectra between IMF B_z and tail B_x for each crossing. It can be seen that main periodicities for the cross-correlation occur from 1.8 to 3.1 h.

One remarkable result of this study is shown in detail for the T2 and T5 tail crossings (Figs. 4 to 9) which exhibits the highest agreement in the period of the strongest power on the cross-wavelet analysis between widely separated regions and between different diagnostics of the substorm process (magnetic field variations/dipolarizations and energetic particle responses/injections). For the T2 crossing the periods range from 2.1 to 2.6 h, while for the T5 crossing periods range from 2.7 to 3.5 h. This similarity on the response of particle and magnetic field variations argues strongly for the global organizing capability of the Alfvénic solar wind fluc-

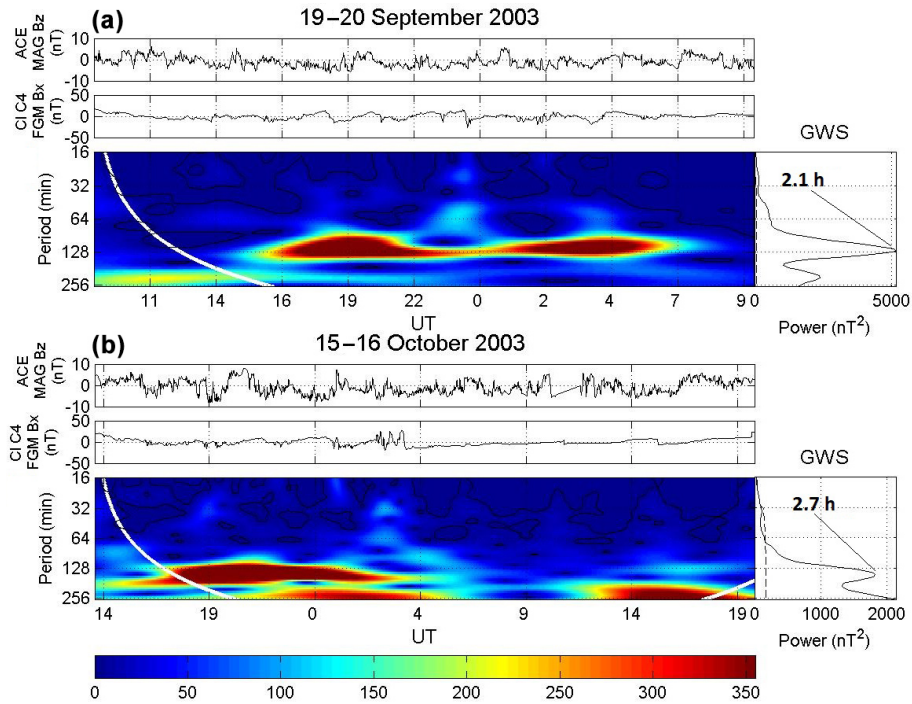


Figure 4. Cross-wavelet spectrum between ACE IMF B_z component and Cluster C4 B_x component for the (a) 19–20 September 2003 tail crossing (T2) and for the (b) 15–16 October 2003 tail crossing (T5). The color bar is the same for (a) and (b). The two global spectra (GWS) are shown on the right. The thick white line shows the cone of influence (COI) limits. The cross-wavelet analysis confidence level of 95 % is marked by black lines in the wavelet plot. Continuous wavelet spectrum background from red noise models is indicated in the GWS plot as a dotted black line, which for very low noise levels may not be visible in subsequent figures as the power range plotted changes in each figure.

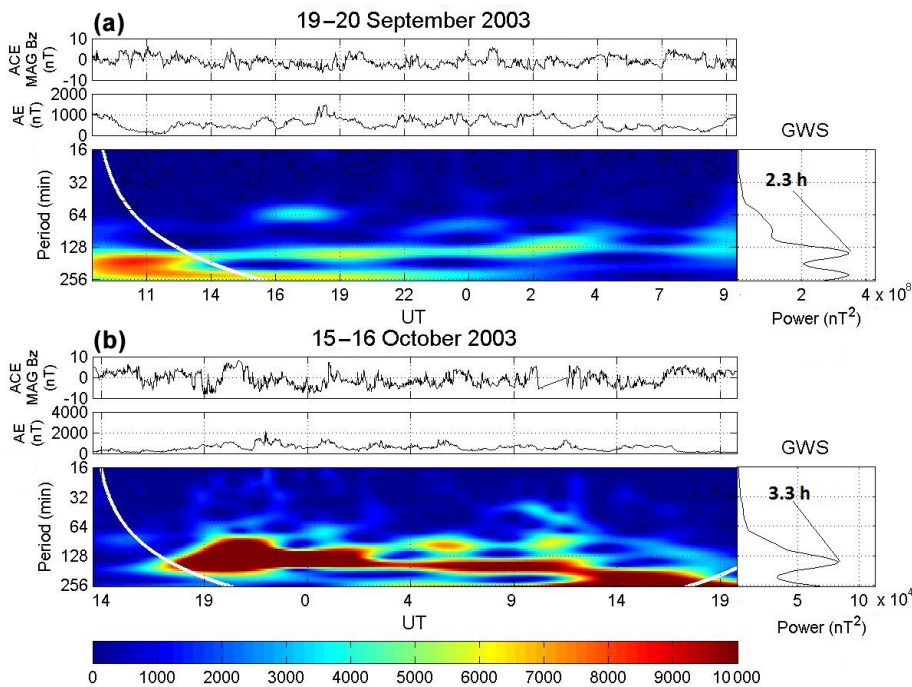


Figure 5. Cross-wavelet spectra between ACE IMF B_z component data and AE index for the (a) 19–20 September 2003 tail crossing (T2) and for the (b) 15–16 October 2003 tail crossing (T5). Otherwise the format is the same as for Fig. 4.

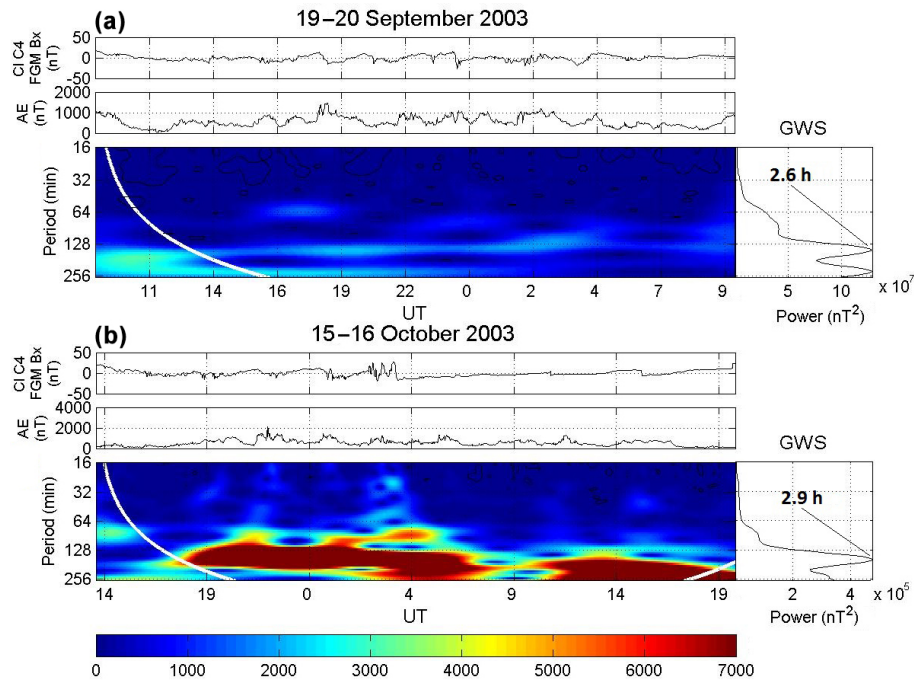


Figure 6. Cross-wavelet spectra between Cluster B_x component data and AE index for the (a) 19–20 September 2003 tail crossing (T2) and for the (b) 15–16 October 2003 tail crossing (T5). Otherwise the format is the same as for Fig. 4.

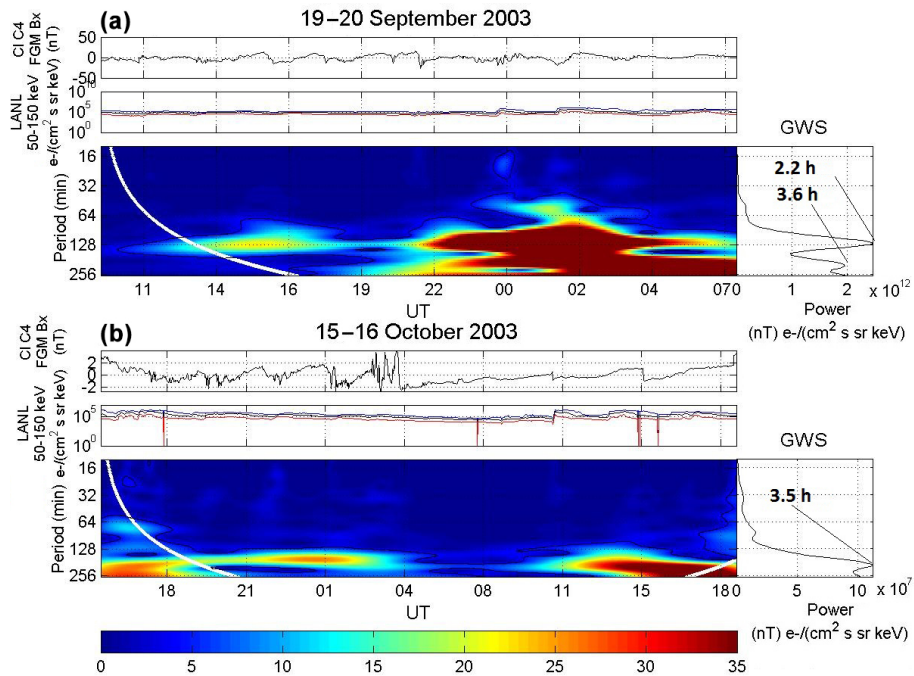


Figure 7. Cross-wavelet spectra between Cluster B_x component data and three LANL electron channels for the (a) 19–20 September 2003 tail crossing (T2) and for the (b) 15–16 October 2003 tail crossing (T5). Otherwise the format is the same as Fig. 4.

tuations in driving a substorm response across large parts of the magnetosphere.

Figure 10 shows the wavelet spectra of the IMF B_z for the two tail crossings previously shown, 19–20 September 2003 and 15–16 October 2003. These plots help determine which

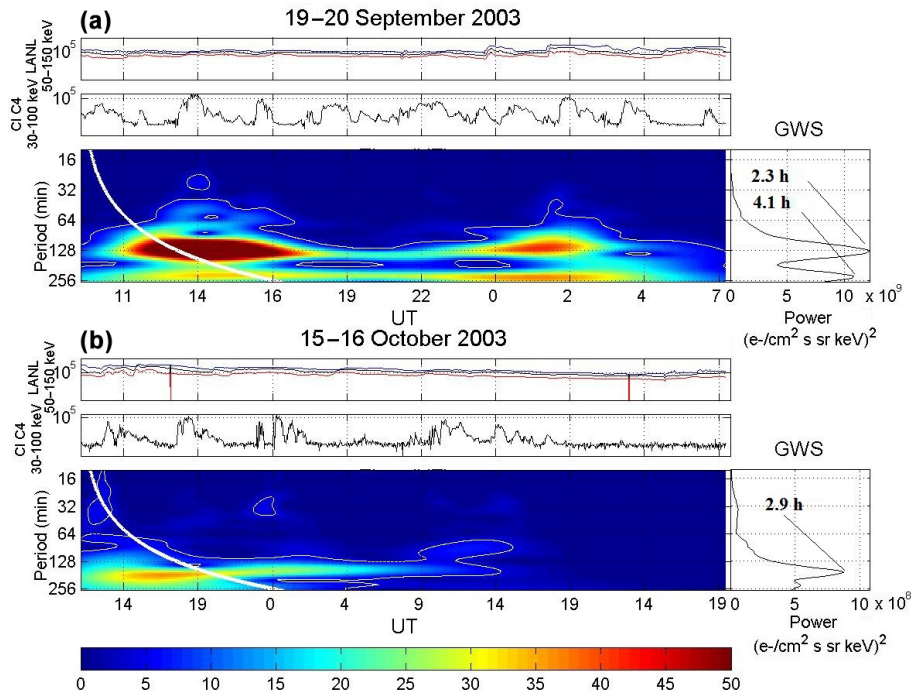


Figure 8. Cross-wavelet spectra between Cluster RAPID >100 keV electron data and three LANL electron channels for the (a) 19–20 September 2003 tail crossing (T2) and for the (b) 15–16 October 2003 tail crossing (T5). Otherwise the format is the same as for Fig. 4.

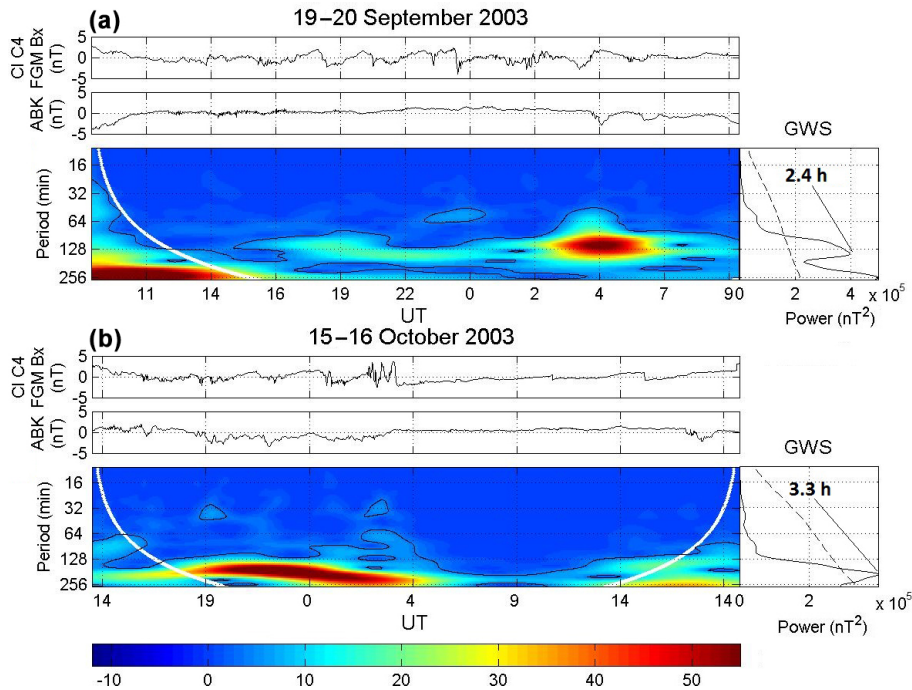


Figure 9. Cross-wavelet spectra between Cluster B_x component data and ABK (Abisko) ground station geomagnetic data for the (a) 19–20 September 2003 tail crossing (T2) and for the (b) 15–16 October 2003 tail crossing (T5). Otherwise the format is the same as for Fig. 4.

periodicities are in the solar wind driver versus the dominant frequencies across the magnetosphere. For the wavelet plot

of B_z during 19–20 September 2003, the main periodicities are ~ 1.0 , 2.4 and 4.2 h. Only the period near 2.4 h was ob-

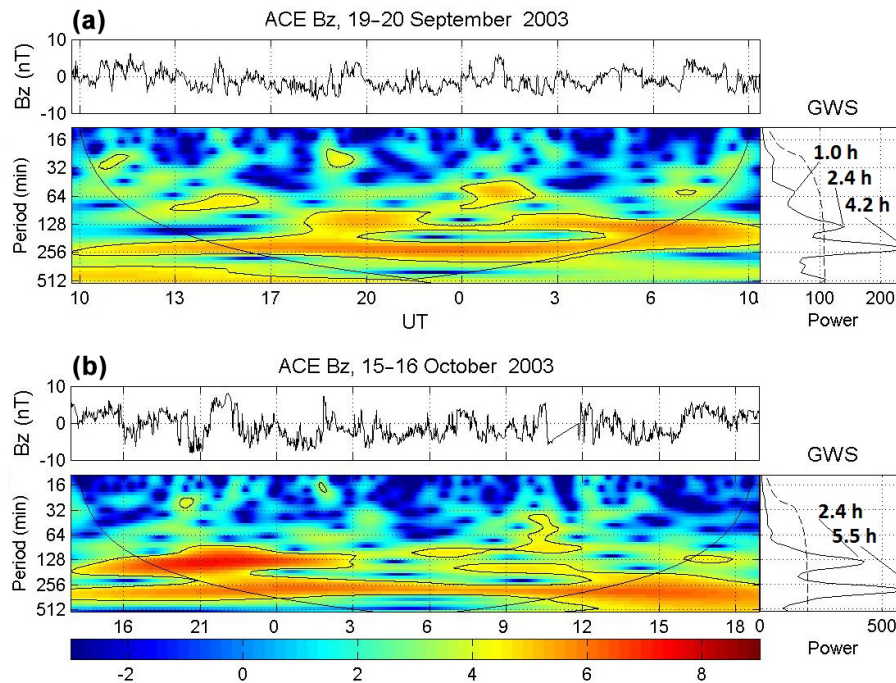


Figure 10. Wavelet spectra of the IMF B_z component for the (a) 19–20 September 2003 tail crossing (T2) and for the (b) 15–16 October 2003 tail crossing (T5). The paraboloidal black line curve is the COI. Regions in the wavelet spectrum with confidence level at 95 % are marked with black lines. Continuous wavelet spectrum background from red noise models shown in the GWS as a black dotted line.

served in the coupling between solar wind–magnetosphere (2.1 h in Fig. 4). For the IMF B_z during 15–16 October 2003, the main periods found in B_z are 2.4 and 5.5 h, while the dominant period in the solar wind tail coupling is at 2.7 h (Fig. 4).

For all the events, the IMF B_z wavelet spectra have a larger spread in periodicities, ranging from ~ 1 to ~ 6.1 h. Major IMF B_z periods range from ~ 1.8 to ~ 5.8 h, and they usually show two peaks one in the range from 1.7 to 2.7 h and the second around 4.2 to 6.2 h.

Comparing IMF B_z and tail B_x wavelet spectra, we found the major periods to be, respectively, as follows (in order of decreasing power): T1 (2.81, 1.875 and 1.27 h; 5.23 and 2.02 h); T2 (4.15, 2.41 and 1.05 h; 2.19, 3.84 and 5.88 h); T3 (5.15, 2.98 and 0.71 h; 2.76 h); T4 (2.76 and 0.97 h; 4.57 and 2.76 h); T5 (5.45 and 2.43 h; 3.19 h); T6 (5.82 and 1.72 h; 5.03, 3.20 and 1.03 h); T7 (1.83 and 6.17 h; 4.39 and 2.25 h). Recent remote sensing inner heliospheric work suggests some periodicity in density inhomogeneities in the solar wind with a period of ~ 90 min (Viall and Vourlidas, 2015), but for slow solar wind. Here in this paper we have found similar periods, but for HSSs.

These results show that the magnetotail system is probably directly driven for the repetitive substorm events studied in this paper, but not all of the IMF periodicities are present in the magnetotail. This means that the magnetosphere filters periods other than the dominant ones that correspond to the characteristic loading/unloading response of the system.

Nevertheless, one cannot conclude that a direct relationship between solar wind forcing and magnetospheric response during substorms exists only by finding similar periods across these regions. This is because of the largely disparate physical character of these domains and the nonlinearities in the magnetospheric response to the solar wind input (Pulkkinen et al., 2007).

Vörös (2000), using the multi-fractal approach on high-latitude geomagnetic fluctuations time series, found an important timescale around 60 min. According to (Benzi and Biferale, 2009), the multi-fractal approach to turbulence is based on the hypotheses that the statistical properties of the turbulent time series do exhibit scaling properties. They stated that this 60 min scale is due to the loading–unloading mechanism, which depends on the geomagnetic activity level. Thus, the period range of 1.8 to 3.1 h (encompassing the 2.75 h from Borovsky et al., 1993) would be a cyclic response of an out of equilibrium system, as the magnetosphere should be. However, more research is necessary in order to better understand the scaling properties of the solar wind turbulence at ~ 1 AU (e.g., Borovsky and Funsten, 2003; Alexandrova et al., 2009; Owens et al., 2014).

There are important differences between the work done by Borovsky (1993) and our present study. Borovsky found the statistical distribution of inter-substorm times for all conditions (active and quiet) and for all types of geomagnetic disturbances. Our study concentrates on a specific subset of events such as HSSs which result in a series of many (~ 4

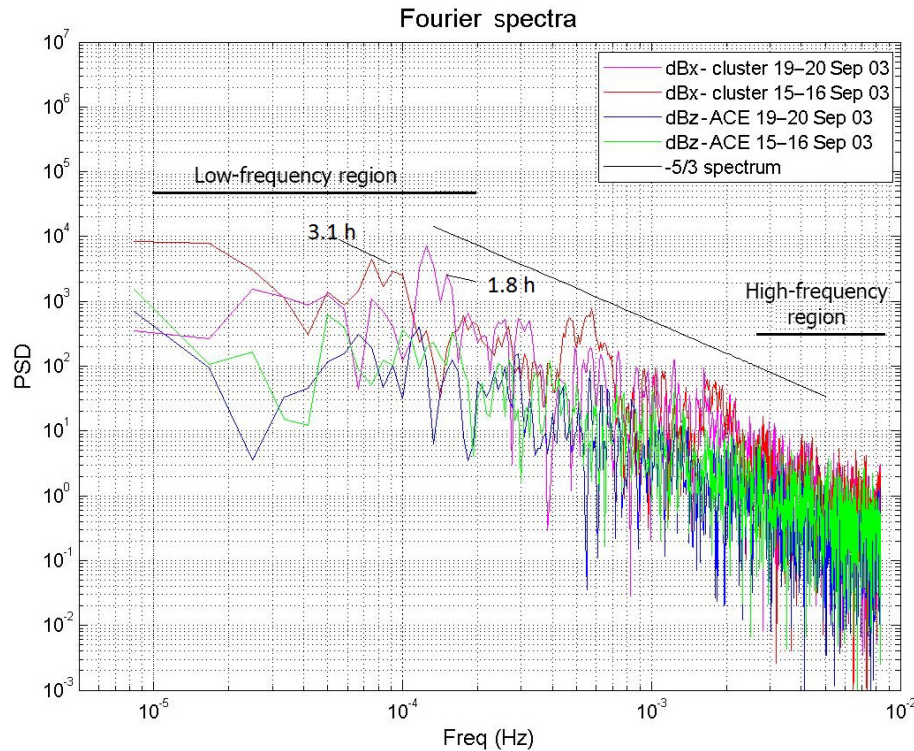


Figure 11. The Fourier spectra from ACE IMF B_z and Cluster tail B_x , obtained in two distinct periods, 19 to 20 September and 15 to 16 October 2003. The black line represents the Kolmogorov's power-law scale of $-5/3$. PSD stands for power spectral density.

to 6) periodic substorms. The majority of the events in the Borovsky study are due to the times between two independent substorms that are *not* part of a longer series. The 2.75 h peak in the Borovsky distribution is quite narrow with a full width at half maximum of ~ 3 h. Our study does not have sufficient events to establish a statistical distribution with any confidence. We note that the major periods found here have an average of 2.4 h and a distribution that spans only 1.3 h. This seems to indicate that for these possibly directly driven HSS-type events studied in this work the magnetosphere is only capable of responding within a narrower set of periods.

Finally, it should be noted that other solar wind parameters (e.g., solar wind speed, density) may have an important role in substorm physics through viscous interaction processes (e.g., Newell et al., 2013). The correlation between those solar wind parameters and magnetospheric parameters during substorms should be examined in future works.

3.4 Test of red noise and white noise effects

Recently some papers have emphasized the importance of discussion of white noise (with a flat Fourier spectrum) and red noise (increasing power with decreasing frequency) in conjunction with the validation of the null hypothesis in order to verify the real main periodicities and amplitudes found in time series (Torrence and Compo, 1998; Alexandrova et al., 2009). The white noise and the red noise are important as-

pects to observers when performing the wavelet and Fourier spectra due to their impact on the scales we are looking for. According to Alexandrova et al. (2009), red noise plays an important role on the spectral analysis and has instrumental origin. Another important aspect is due to different wavelet functions which could compromise the identification of temporal variability of each periodicity found. Bolzan et al., 2006 observed that different wavelet functions may cause different behavior on the extraction of the coherent structures (CSs). Indeed, different wavelet functions cause different behavior on the white noise and red noise present in different time series. Bolzan et al. (2009), using two kinds of wavelet function in order to extract the CSs, have shown that each wavelet has a different performance due to its mathematical shape. Thus it is possible to assess how different wavelet functions when applied to the same observation data, and taking into account the noise, may lead to different results.

However, it is important to note the presence of the universal characteristics for different plasma conditions and solar wind regimes (Alexandrova et al., 2009). One such universal characteristic is due to the presence of the Kolmogorov's $-5/3$ power-law scale, which is commonly observed in turbulent flows in distinct environments, hydrodynamical (HD) and magnetohydrodynamical (MHD). Alexandrova et al. (2009) mentioned that the white noise and red noise are predominant in high frequencies; some low fre-

quencies are not affected. Auchère et al. (2016) showed concern about the power-law dependence of the power spectra of time series from geophysical data. Thus, in order to better examine this issue, Fig. 11 shows the Fourier spectrum from ACE IMF B_z and Cluster tail B_x during two distinct intervals from 19 to 20 September and 15 to 16 October 2003. It is possible to note the main periodicities found in this work (1.8 up to 3.1 h) are far from the high frequencies as mentioned by Alexandrova et al. (2009; frequencies $> 10^{-4}$ Hz, see Fig. 11). Thus, the influence of the red noise and white noise does not affect the periods found according to the Fig. 11.

Furthermore, we calculated the red noise based on the Markov process, according to Torrence and Compo (1998). However, we did not plot the continuous wavelet spectrum (CWS) background in all Figs. 4 to 10, and we can observe the presence of the dashed line of the CWS background in GWS plots only in some specific cases such as in Figs. 4, 9 and 10. Nevertheless, we noted that all periodicities found are not affected by the red noise.

4 Conclusions

In this work, we have studied the coupling from solar wind at 1 AU to the magnetotail to geosynchronous orbit to ground during the HSS/CIR intervals in September/October 2003. Cross-wavelet analysis was employed to compare several time series across the magnetosphere. We have obtained major periods of 1.8 to 3.1 h for the solar wind–magnetosphere energy coupling during those HSSs which are within the range of a typical substorm period. The coupling frequencies were remarkably globally consistent between different regions: magnetotail, geosynchronous orbit, the auroral region and the ground, and across both magnetic and particle flux variations. This period range encompasses the 2.75 h peak from Borovsky et al. (1993), distribution of inter-substorm times (that had a broad peak from 2 to 4 h, encompassing most of the periods found in this work). However, our observed range of periods (1.3 h) is less broad than the 3 h width of the peak in the Borovsky study. This might indicate a more restricted magnetospheric frequency response in possibly driven events such as the HSS cases of this study. Overall the global behavior is a cyclic response of an out of equilibrium system, as the magnetosphere should be.

Data availability. Solar wind data are freely available from the NASA/GSFC Omniweb server (<https://omniweb.gsfc.nasa.gov/>). Cluster data are available from the ESAC Cluster science archive (<https://www.cosmos.esa.int/web/csa>). AE, Dst and ground-based data are available from the WDC Kyoto Data Centre for Geomagnetism (wdc.kugi.kyoto-u.ac.jp/). LANL energetic particle data are available through <http://www.mpa.lanl.gov/data.shtml>.

Competing interests. The authors declare that they have no conflict of interest.

Acknowledgements. Ezequiel Echer acknowledges the Brazilian CNPQ agency contract number PQ-302583/2015-7 for support for this work. M. J. A. Bolzan also acknowledges the CNPQ agency contract no. PQ-303103/2012-4 and FAPESP agency contract no. 2012.1026.7000905. Axel Korth was supported by the Max-Planck-Gesellschaft zur Förderung der Wissenschaften and the Bundesministerium für Bildung und Forschung (BMFT) under grant 50 OC 0801. Axel Korth would like to thank the PIs and teams of the Cluster CIS, RAPID and FGM instruments.

The topical editor, Georgios Balasis, thanks Ramon E. Lopez and two anonymous referees for help in evaluating this paper.

References

- Akasofu, S.-I.: The development of auroral substorm, *Planet. Space Sci.*, 12, 273–282, 1964.
- Akasofu, S.-I.: Energy coupling between the solar wind and the magnetosphere, *Space Sci. Rev.*, 28, 121–190, 1981.
- Alexandrova, O., Saur, J., Lacombe, C., Mangeney, A., Mitchell J., Schwartz, S. J., and Robert, P.: Universality of solar-wind turbulent spectrum from MHD to electron scales, *Phys. Rev. Lett.*, 103, 4 pp., 2009.
- Alves, M. V., Echer, E., and Gonzalez, W. D.: Geoeffectiveness of corotating interaction regions as measured by Dst index, *J. Geophys. Res.*, 111, A07S05, <https://doi.org/10.1029/2005JA011379>, 2006.
- Angelopoulos, V., McFadden, J. P., Larson, D., Charles W. Carlson, C. W., Mende, S. B., Mende Frey, H., Phan, T., Sibeck, D. G., Glassmeier, K.-H., Auster, U., Donovan, E., Mann, I. R., Rae, I. J., Russell, C. T., Runov, A., Zhou, X.-Z., and Kepko, L.: Tail reconnection triggering substorm onset, *Science*, 321, 931–935, <https://doi.org/10.1126/science.1160495>, 2008.
- Auchère, F., Froment, C., Bocchialini, K., Buchlin, E., and Solomon, J.: On the Fourier and wavelet analysis of coronal time series, *Astrophys. J.*, 825, 1–13, 2016.
- Baker, D.: Solar wind-magnetosphere drivers of space weather, *J. Atmos. Terr. Phys.*, 58, 1509–1526, 1996.
- Baker, D. N., Pulkkinen, T. I., Angelopoulos, V., Baumjohann, W., and McPherron, R. L.: Neutral line model of substorms: Past results and present view, *J. Geophys. Res.*, 101, 12975–13010, 1996.
- Baker, D., McPherron, R. L., and Dunlop, M. W.: Cluster observations of magnetospheric substorm behaviour in the near- and mid-tail region, *Adv. Space Res.*, 36, 1809–1817, 2005.
- Balasis, G., Daglis, I. A., Kapisiris, P., Manda, M., Vassiliadis, D., and Eftaxias, K.: From pre-storm activity to magnetic storms: a transition described in terms of fractal dynamics, *Ann. Geophys.*, 24, 3557–3567, <https://doi.org/10.5194/angeo-24-3557-2006>, 2006.
- Balasis, G., Daglis, I. A., Papadimitriou, C., Kalimeri, M., Anastasiadis, A., and Eftaxias, K.: Investigating dynamical complexity in the magnetosphere using various entropy measures, *J. Geophys. Res.*, 114, A00D06, <https://doi.org/10.1029/2008JA014035>, 2009.

- Balasis, G., Daglis, I. A., Zesta, E., Papadimitriou, C., Georgiou, M., Haagmans, R., and Tsinganos, K.: ULF wave activity during the 2003 Halloween superstorm: multipoint observations from CHAMP, Cluster and Geotail missions, *Ann. Geophys.*, 30, 1751–1768, <https://doi.org/10.5194/angeo-30-1751-2012>, 2012.
- Balogh, A., Bothmer, V., Crooker, N. U., Forsyth, R. J., Gloeckler, G., Hewish, A., Hilchenbach, M., Kallenbach, R., Klecker, B., Linker, J. A., Lucek, E., Mann, G., Marsch, E., Posner, A., Richardson, I. G., Schmidt, J. M., Scholer, M., Wang, Y.-M., Wimmer-Schweingruber, R. F., Aellig, M. R., Bochler, P., Hefti, S., and Mikic, Z.: The solar origin of corotating interaction regions and their formation in the inner heliosphere, *Space Sci. Rev.*, 89, 147–178, 1999.
- Balogh, A., Carr, C. M., Acuña, M. H., Dunlop, M. W., Beek, T. J., Brown, P., Fornacon, K.-H., Georgescu, E., Glassmeier, K.-H., Harris, J., Musmann, G., Oddy, T., and Schwingenschuh, K.: The Cluster Magnetic Field Investigation: overview of in-flight performance and initial results, *Ann. Geophys.*, 19, 1207–1217, <https://doi.org/10.5194/angeo-19-1207-2001>, 2001.
- Bame, S. J., McComas, D. J., Young, D. T., and Belian, R. D.: Diagnostics of space plasmas, *Rev. Sci. Instrum.*, 57, 1711, <https://doi.org/10.1063/1.1138558>, 1986.
- Belcher, J. W. and Davis Jr., L.: Large Amplitude Alfvén waves in the interplanetary medium, *J. Geophys. Res.*, 76, 3534–3563, 1971.
- Benzi, R. and Biferale, L.: Fully Developed Turbulence and the Multifractal Conjecture, *J. Stat. Phys.*, 135, 977–990, <https://doi.org/10.1007/s10955-009-9738-9>, 2009.
- Blanchard, G. T., Lyons, L. R., and Spann, J.: Predictions of substorms following northward turnings of the interplanetary magnetic field, *J. Geophys. Res. Pt. A*, 105, 375–384, 2000.
- Bolzan, M. J. A. and Vieira, P. C.: Wavelet analysis of the wind velocity and temperature variability in the Amazon forest, *Braz. J. Phys.*, 36, 1217–1222, <https://doi.org/10.1590/S0103-97332006000700018>, 2006.
- Bolzan, M. J. A., Guarnieri, F. L., and Vieira, P. C.: Comparisons between two wavelet functions in extracting coherent structures from solar wind time series, *Braz. J. Phys.*, 39, 12–17, <https://doi.org/10.1590/S0103-97332009000100002>, 2009.
- Bolzan, M. J. A., Echer, E., and Korth, A.: Cross-wavelet analysis on the interplanetary and magnetospheric tail magnetic field data, *Proceedings XXXIV Congresso Nacional de Matemática Aplicada e Computacional, Águas de Lindóia, Brazil*, 797–802, 2012.
- Borovsky, J. E. and Funsten, H. O.: Role of solar wind turbulence in the coupling of the solar wind to the Earth's magnetosphere, *J. Geophys. Res.*, 108, 1246, <https://doi.org/10.1029/2002JA009601>, 2003.
- Borovsky, J. E., Nemzek, R. J., and Belian, R. D.: The occurrence rate of magnetospheric substorm onsets: Random and period substorms, *J. Geophys. Res.*, 98, 3807–3813, 1993.
- Burch, J. L.: Plasma populations in the magnetosphere, in: *The Solar Wind and the Earth*, edited by: Akasofu, S.-I. and Kamide, Y., Terra Scientific Publishing Company (TERRAPUB), Tokyo, Chap. 6, 1987.
- Burlaga, L. F. and Lepping, R. P.: The cause of recurrent geomagnetic storms, *Planet. Space Sci.*, 25, 1151–1160, 1977.
- Cranmer, S. R.: Coronal Holes, *Living Reviews in Solar Physics*, 6, 66 pp., <https://doi.org/10.12942/lrsp-2009-3>, 2009.
- Crooker, N. U. and Cliver, E. W.: Postmodern view of M-regions, *J. Geophys. Res.*, 99, 23383–23390, 1994.
- Davis, T. N. and Sugiura, M.: Auroral electrojet activity index AE and its universal time variations, *J. Geophys. Res.*, 71, 785–801, 1966.
- Dungey, J. W.: Interplanetary magnetic field and the auroral zones, *Phys. Rev. Lett.*, 6, 47–48, <https://doi.org/10.1103/PhysRevLett.6.47>, 1961.
- Echer, E., Gonzalez, W. D., Guarnieri, F. L., Dal Lago, A., and Vieira, L. E. A.: Introduction to Space Weather, *Adv. Space Res.*, 35, 855–865, <https://doi.org/10.1016/j.asr.2005.02.098>, 2005.
- Echer, E., Gonzalez, W. D., Tsurutani, B. T., and Gonzalez, A. L. C.: Interplanetary conditions causing intense geomagnetic storms ($Dst \leq 100$ nT) during solar cycle 23 (1996–2006), *J. Geophys. Res.*, 113, A05221, <https://doi.org/10.1029/2007JA012744>, 2008.
- Echer, E., Gonzalez, W. D., and Tsurutani, B. T.: Statistical studies of geomagnetic storms with peak $Dst \leq -50$ nT from 1957 to 2008, *J. Atmos. Sol.-Terr. Phys.*, 73, 1454–1459, 2011.
- Echer, E., Tsurutani, B. T., and Gonzalez, W. D.: Interplanetary origins of moderate (-100 nT $< Dst \leq -50$ nT) geomagnetic storms during solar cycle 23 (1996–2008), *J. Geophys. Res.*, 118, 385–392, 2013.
- Freeman, M. P. and Morley, S. K.: A minimal substorm model that explains the observed statistical distribution of times between substorms, *Geophys. Res. Lett.*, 31, 1–4, 2004.
- Freeman, M. P. and Morley, S. K.: No evidence for externally triggered substorms based on superposed epoch analysis of IMF B_z , *Geophys. Res. Lett.*, 36, 1–4, 2009.
- Gonzalez, W. D., Joselyn, J. A., Kamide, Y., Kroehl, H. W., Rosotoker, G., Tsurutani, B. T., and Vasyliunas, V. M.: What is a geomagnetic storm?, *J. Geophys. Res.*, 99, 5771–5792, 1994.
- Gonzalez, W. D., Tsurutani, B. T., and Clua de Gonzalez, A. L.: Interplanetary origin of geomagnetic storms, *Space Sci. Rev.*, 88, 529–62, <https://doi.org/10.1023/A:1005160129098>, 1999.
- Gonzalez, W. D., Echer, E., Clua-Gonzalez, A. L., and Tsurutani, B. T.: Interplanetary origin of intense geomagnetic storms ($Dst < -100$ nT) during solar cycle 23, *Geophys. Res. Lett.*, 34, L06101, <https://doi.org/10.1029/2006GL028879>, 2007.
- Gonzalez, W. D., Echer, E., Tsurutani, B. T., Clúa de Gonzalez, A. L., and Dal Lago, A.: Interplanetary origin of intense, superintense and extreme geomagnetic storms, *Space Sci. Rev.*, 158, 69–89, 2011.
- Gosling, J. T. and Pizzo, V. J.: Formation and evolution of corotating interaction regions and their three dimensional structure, *Space Sci. Rev.*, 89, 21–52, 1999.
- Guarnieri, F. L., Tsurutani, B. T., Gonzalez, W. D., Echer, E., Gonzalez, A. L. C., Grande, M., and Soraas, F.: ICME and CIR storms with particular emphasis on HILDCAA events, in: *The Solar Influence on the Heliosphere and Earth's Environment: Recent Progress and Prospects*, edited by: Gopalswamy, N. and Bhattacharyya, A., 19–24, 2006a.
- Guarnieri, F. L., Tsurutani, B. T., Echer, E., and Gonzalez, W. D.: Geomagnetic activity and auroras caused by high-speed streams: A review, *Advances in Geosciences*, in: *Solar-Terrestrial*, edited by: Dulig, M., World Scientific CO, Pte. Ltd, Singapore, 2006., 8, p. 91, 2006b.
- Hajra, R., Echer, E., Tsurutani, B. T., and Gonzalez, W. D.: Solar cycle dependence of High-Intensity Long-Duration

- Continuous AE Activity (HILDAA) events, relativistic electron predictors?, *J. Geophys. Res.*, 118, 5626–5638, <https://doi.org/10.1002/jgra.50530>, 2013.
- Henderson, M. G., Murphree, J. S., and Weygand, J. M.: Observations of auroral substorms occurring together with preexisting “quiet time” auroral patterns, *J. Geophys. Res.*, 101, 24621–24640, <https://doi.org/10.1029/96JA01252>, 1996.
- Hollweg, J. V.: Some physical processes in the solar wind, *Rev. Geophys. Space Phys.*, 16, 687–720, 1978.
- Kamide, Y., Baumjohann, W., Daglis, A., Gonzalez, W. D., Grande, M., Joselyn, J. A., McPherron, R. L., Phillips, J. L., Reeves, E. G. D., Rostoker, G., Sharma, A. S., Singer, H. J., Tsurutani, B. T., and Vasyliunas, V. M.: Current understanding of magnetic storms: Storm-substorm relationships, *J. Geophys. Res.*, 103, 17705–17728, <https://doi.org/10.1029/98JA01426>, 1998.
- Katsavrias, Ch., Hillaris, A., and Preka-Papadema, P. A.: wavelet based approach to Solar-Terrestrial Coupling, *Adv. Space Res.*, 57, 2234–2244, 2016.
- Korth, A., Echer, E., Guarnieri, F. L., Fränz, M., Friedel, R., Gonzalez, W. D., Mouikis, C. G., and Rème, H.: Cluster observations of plasma sheet activity during the September 14–28, 2003 corotating high speed stream event, *Proceedings of the Eight International Conference on Substorms (ICS-8)*, edited by: Syrjäso, M. and Donovan, E., Univ. Calgary, Canada, 8, 133–138, 2006.
- Kozyra, J. U., Crowley, G., Emery, B. A., Fang, X., Maris, G., Mlynczak, M. G., Niciejewski, R. J., Palo, S. E., Paxton, L. J., Randall, C. E., Rong, P.-P., Russell III, J. M., Skinner, W., Solomon, S. C., Talaat, E. R., Wu, Q., and Yee, J.-H.: Response of the upper/middle atmosphere to coronal holes and powerful high speed solar wind streams in 2003, in: *Recurrent Magnetic Storms: Corotating Solar Wind Streams*, *Geophys. Monogr. Ser.*, edited by: Tsurutani, B. T., McPherron, R. L., Gonzalez, W. D., Lu, G., Sobral, J. H. A., and Gopalswamy, N., AGU, Washington, DC, 319–340, 2006.
- Kumar, P., and Foufoula-Georgiou, E.: Wavelet analysis for geophysical applications, *Rev. Geophys.*, 35, 385–412, 1997.
- Lee, D.-Y., Lyons, L. R., Kim, K. C., Baek, J.-H., Kim, K.-H., Kim, H.-J., Weygand, J., Moon, Y.-J., Cho, K.-S., Park, Y. D., and Han, W.: Repetitive substorms caused by Alfvénic waves of the interplanetary magnetic field during high-speed wind streams, *J. Geophys. Res.*, 111, 14 pp., <https://doi.org/10.1029/2006JA011685>, 2006.
- Lindsay, G. M., Russell, C. T., and Luhmann, J. G.: Coronal mass ejection and stream interaction region characteristics and their potential geoeffectiveness, *J. Geophys. Res.*, 100, 16999–17013, 1995.
- Lui, A. T. Y.: Current disruption in the Earth’s magnetosphere: Observations and models, *J. Geophys. Res.*, 101, 13067–13088, 1996.
- Lui, A. T. Y., Zheng, Y., Reme, H., and Dunlop, M. W.: Evaluation of substorm models with Cluster observations of plasma flow reversals in the magnetotail, *Adv. Space Res.*, 41, 1611–1618, 2008.
- Lyons, L. R., Lee, D.-Y., Kim, H.-J., Hwang, J. A., Thorne, R. M., Horne, R. B., and Smith, A. J.: Solar wind-magnetosphere coupling, including relativistic electron energization, during high-speed streams, *J. Atmos. Sol.-Terr. Phys.*, 71, 1059–1072, <https://doi.org/10.1016/j.jastp.2008.04.016>, 2009.
- McComas, D. J., Bame, S. J., Baker, P., Feldman, W. C., Phillips, J. L., Riley, P., and Griffée, J. W.: Solar wind electron proton alpha monitor (SWEPAM) for the advanced composition explorer, *Space Sci. Rev.*, 86, 563–612, 1998.
- Morley, S. K. and Freeman, M. P.: On the association between northward turnings of the interplanetary magnetic field and substorm onsets, *Geophys. Res. Lett.*, 34, 1–6, 2007.
- Newell, P. T., Gjerloev, J. W., and Mitchell, E. J.: Space climate implications from substorm frequency, *J. Geophys. Res.*, 118, 6254–6265, <https://doi.org/10.1002/jgra.50597>, 2013.
- Owens, M. J., Horbury, T. S., Wicks, R. T., McGregor, S. L., Savani, N. P., and Xiong, M.: Ensemble downscaling in coupled solar wind-magnetosphere modelling for space weather forecast, *Space Weather*, 12, 395–405, <https://doi.org/10.1002/2014SW001064>, 2014.
- Percival, D. B. and Walden, A. T.: *Wavelet Methods for Time Series Analysis*, Cambridge University Press, Cambridge, 2000.
- Pizzo, V.: A three-dimensional model of corotating streams in the solar wind, 3 Magnetohydrodynamic streams, *J. Geophys. Res.*, 87, 4374–4394, 1982.
- Pulkkinen, T. I., Partamies, N., McPherron, R. L., Henderson, M., Reeves, G. D., Thomsen, M. F., and Singer, H. J.: Comparative statistical analysis of storm time activations and sawtooth events, *J. Geophys. Res.*, 112, A01205, <https://doi.org/10.1029/2006JA012024>, 2007.
- Reme, H. and CIS Team: First multispacecraft ion measurements in and near the Earth’s magnetosphere with the identical Cluster Ion Spectrometry (CIS) experiment, *Ann. Geophys.*, 19, 1303–1354, 2001.
- Richardson, I. G., Cliver, E. W., and Cane, H. V.: Sources of geomagnetic activity over the solar cycle: Relative importance of coronal mass ejections, high-speed streams and slow solar wind, *J. Geophys. Res.*, 105, 18203–18213, 2000.
- Rostoker, G.: *Geomagnetic Indices*, *Rev. Geophys.*, 10, 935–950, 1972.
- Rostoker, G., Akasofu, S. I., Foster, J., Greenwald, R. A., Kamide, Y., Kawasaki, K., Lui, A. T. Y., McPherron, R. L., and Russell, C. T.: Magnetospheric substorms – definitions and signatures, *J. Geophys. Res.*, 85, 1663–1668, 1980.
- Russell, C. T., McPherron, R. L., and Burton, R. K.: On the cause of geomagnetic storms, *J. Geophys. Res.*, 79, 1105–1110, 1974.
- Sergeev, V. A.: Energetic particles as tracers of magnetospheric configuration, *Adv. Space Res.*, 18, 161–170, 1996.
- Sheeley, N. R., Harvey Jr., J. W., and Feldman, W. C.: Coronal holes, solar wind streams, and recurrent geomagnetic disturbances, *Solar Phys.*, 49, 271–278, 1976.
- Smith, E. J. and Wolfe, J. H.: Observations of interaction regions and corotating shocks between one and 5 AU – Pioneer-10 and Pioneer-11, *Geophys. Res. Lett.*, 3, 137–140, 1976.
- Smith, C. W., Acuna, M. H., Burlaga, L. F., Heures, J. L., Ness, N. F., and Scheifele, J.: The ACE magnetic field experiment, *Space Sci. Rev.*, 86, 613–632, 1998.
- Tanskanen, E. I., Slavin, J. A., Tanskanen, A. J., Viljanen, A., Pulkkinen, T. I., Koskinen, H. E. J., Pulkkinen, A., and Eastwood, J.: Magnetospheric substorms are strongly modulated by interplanetary high-speed streams, *Geophys. Res. Lett.*, 32, L16104, <https://doi.org/10.1029/2005GL023318>, 2005.
- Torrence, C. and Compo, G. P.: A Practical Guide to Wavelet Analysis, *B. Am. Meteorol. Soc.*, 79, 61–78, 1998.

- Tsurutani, B. T. and Meng, C. I.: Interplanetary magnetic field variations and activity, *J. Geophys. Res.*, 77, 2964–2970, 1972.
- Tsurutani, B. T., Gonzalez, W. D., Gonzalez, A. L. C., Tang, F., Arballo, J. K., and Okada, M.: Interplanetary origin of geomagnetic activity in the declining phase of the solar cycle, *J. Geophys. Res.*, 100, 21717–21733, 1995.
- Tsurutani, B. T., Gonzalez, W. D., Gonzalez, A. L. C., Guarnieri, F. L., Gopalswamy, N., Grande, M., Kamide, Y., Kasahara, Y., Lu, G., Mann, I., McPherron, R., Soraas, F., and Vasyliunas, V.: Corotating solar wind streams and recurrent geomagnetic activity: A review, *J. Geophys. Res.*, 111, 1–25, <https://doi.org/10.1029/2005JA011273>, 2006.
- Tsurutani, B. T., Echer, E., Guarnieri, F. L., and Gonzalez, W. D.: The properties of two solar wind high speed streams and related geomagnetic activity during the declining phase of solar cycle 23, *J. Atmos. Sol.-Terr. Phys.*, 73, 164–177, 2011.
- Viall, N. M. and Vourlidas, A.: Periodic density structures and the origin of the slow solar Wind, *Astrophys. J.*, 807, 13 pp., <https://doi.org/10.1088/0004-637x/807/2/176>, 2015.
- Vörös, Z.: On multifractality of high-latitude geomagnetic fluctuations, *Ann. Geophys.*, 18, 1273–1282, <https://doi.org/10.1007/s00585-000-1273-6>, 2000.
- Wilken, B., Daly, P. W., Mall, U., Aarsnes, K., Baker, D. N., Belian, R. D., Blake, J. B., Borg, H., Büchner, J., Carter, M., Fennell, J. F., Friedel, R., Fritz, T. A., Gliem, F., Grande, M., Kecskemeti, K., Kettmann, G., Korth, A., Livi, S., McKenna-Lawlor, S., Mursula, K., Nikutowski, B., Perry, C. H., Pu, Z. Y., Roeder, J., Reeves, G. D., Sarris, E. T., Sandahl, I., Søråas, F., Woch, J., and Zong, Q.-G.: First results from the RAPID imaging energetic particle spectrometer on board Cluster, *Ann. Geophys.*, 19, 1355–1366, <https://doi.org/10.5194/angeo-19-1355-2001>, 2001.